SPACE-BASED SHORT RANGE OBSERVATION FOR LEO DEBRIS

Makoto Tagawa[(1)], Toshifumi Yanagisawa[(2)], Haruhisa Matsumoto[(3)], Yukihito Kitazawa[(4)], Toshiya Hanada[(5)]

[(1)] Kyushu University, 744 Moto-oka, Nishi-ku, Fukuoka, 819-0395, Japan, makoto_t@aero.kyushu-u.ac.jp:
[(2)] Japan Aerospace Exploration Agency, 7-44-1 Jindaiji Higashi-machi, Chofu, Tokyo, 182-8522, Japan, tyanagi@chofu.jaxa.jp:
[(3)] Japan Aerospace Exploration Agency, 2-1-1 Sengen, Tsukuba, Ibaraki, 305-8505, Japan, matsumoto.haruhisa@jaxa.jp:
[(4)] IHI Corporation, 3-1-1 Toyosu, Koto-ku, Tokyo, 135-8710, Japan, kitazawa@planeta.sci.isas.jaxa.jp:
[(5)] Kyushu University, 744 Moto-oka, Nishi-ku, Fukuoka, 819-0395, Japan, hanada.toshiya.293@m.kyushu-u.ac.jp:

ABSTRACT

Space debris is one of the major threats for safe and sustainable development and utilizations of space. The orbital object catalog is very important to conduct debris counter measures. However, current database opened to the public has insufficiencies in its tracking size capability. This paper proposes new debris observation system based on space-based sensors. To track the objects observed by the sensors, and maintain their catalog; this paper also proposes collaborative observation with ground sensor networks. This paper mainly discusses on the following topics; 1) mission design for space-based sensors 2) expected values of observation capabilities 3) tracking capability including collaboration with ground facilities. As an initial result, this paper concluded that the combination of a single observation satellite and three ground facilities are able to track approximately 10 % of LEO objects. This paper also summarizes that collaborative observation geometry can cover true apparent motion while quite large field of view is required.

1 INTRODUCTION

Orbital environment has been contaminated with space debris since the first artificial satellite launch in 1957. Present number of objects being tracked is approximately 17,000 (as of February 2013) [1]. The tracked objects catalogue is being opened to the public however; available size of the catalogue is limited to approximately 10 cm in Low Earth Orbit (LEO) [2]. This size limitation means that LEO satellites are able to operate Collision Avoidance Maneuver (CAM) for only 10 cm or larger objects even if the satellites have both of enough powerful motors and amount of propellant. Another satellite-based countermeasure for space debris is to protect core unit from losing function due to debris collision. However, current shielding capability for debris collision is limited to objects smaller than 1 cm [3]. These restrictions in CAM and shielding capabilities conclude that there is no effective solution for 1 to 10 cm debris in LEO. This paper proposes space-based sensors to improve small (1 to 10 cm in size) debris tracking capability furthermore CAM availability for spacecraft in LEO. Space-based sensors are able to ignore negative effect of atmospheric disturbances for observations. There are previous works in space-based debris observation. The Infra-Red Astronomical Satellite (IRAS) launched in 1983 is one of examples and its primary objective is IR survey of celestial sphere for 10 month from altitude 900 km Sun Synchronous Orbit (SSO) [4]. The IRAS operators detected non-celestial objects' tracks in the archived images and they made object catalogue from the images. However their orbit estimation results had distributions in orbital elements plane therefore; the IRAS observation results were hardly applicable for LEO debris catalogue improvement furthermore CAM operation capabilities. Other examples are Space-Based Visible (SBV) equipped on Mid-Course Space Experiment (MSX) satellite and Space-Based Space Surveillance (SBSS) developed by Boeing [5] [6]. Both satellites are mainly designed for Geo stationary Orbit (GEO) survey and application for LEO is limited to orbit data update of catalogued objects. Thus current status for small debris countermeasure is summarized as that there are not operated effective solutions. Proposing space-based sensors have advantages in observation sensitivity in comparison to ground facilities. However, previous study indicates disadvantage of space-based sensors in periodic observation which is essential for catalogue maintenance [7]. This disadvantage comes from observable relative relation limitation in orbital planes. Therefore this paper also proposes collaborative observation geometry between space-based sensors and ground facilities. Basic idea of this geometry is that space-based sensors provide Initial Orbit Determination results using constrained algorithm with very short arc observation to ground facilities and, ground facilities track the objects based on IOD results using image processing algorithm developed to detect faint objects. This paper discusses orbit design for space-based observatory, IOD capability and collaboration feasibility.

Proc. '6th European Conference on Space Debris'
Darmstadt, Germany, 22–25 April 2013 (ESA SP-723, August 2013)

2 MISSION OBJECTIVES AND GEOMETRIES

As mentioned before, final goal is to track 1 to 10 cm objects in LEO, here initial goal is defined as to track 5 cm or larger objects in LEO for preliminary mission design. One of reasons for current insufficiency in LEO small debris tracking is atmosphere. Incident lights from space are extinct by atmospheric layer and observable time is often limited by weather conditions. Space-based sensors can ignore such atmospheric negative effect for observations. Therefore space-based sensors are proposed as LEO tracking capability improvement method in this paper. However, previous study indicates that space-based sensors have disadvantages in periodic observation which is essential to maintain the catalogue, and details are discussed later. Thus this paper also introduces collaborative observation geometry consist of space-based sensors and ground facilities. This proposing geometry based on assumption that an image processing algorithm for faint object called "image stacking method" is applicable for LEO objects. The method makes it is possible to observe objects which are too dark to detect on single image and it has been verified for GEO objects [8].

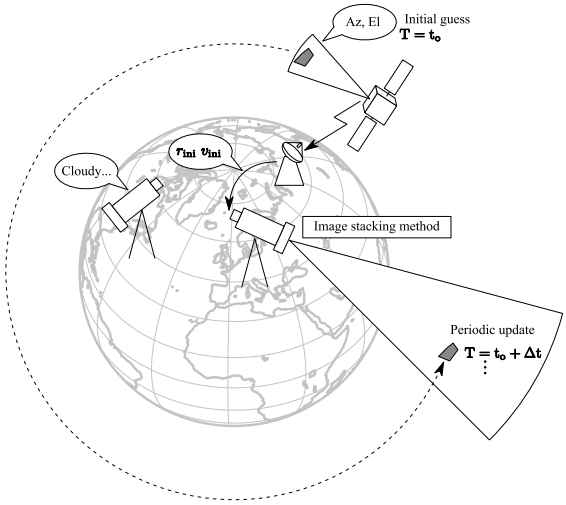

Figure 1. Collaborative observation geometry

Fig 1 illustrates whole observation geometry for LEO small debris tracking mission. The mission is assumed to be separated into two phases; 1) detect small debris using space-based sensors, conduct angles only IOD and provide determined orbit to ground facilities 2) maintain the LEO object catalogue by ground station network. The very first observation in phase 2 requires IOD result to apply the image stacking method. After that catalogue maintenance should be operated by ground facilities only. In short, space-based sensors are used only for initial guess. The LEO to LEO observation geometry is suitable to detect small debris dark enough to being faint from ground however observation capability of space-based sensors is sensitive to relative position and velocity in such short range observation condition. This condition should be considered first to realize the mission therefore this paper mainly discuss phase 1 as a first step to design whole geometry.

2.1 Orbit Design of Space-based Sensors

Space-based sensors are assumed as optical devices because of smaller scale, less power consumption and higher resolution in angles in comparison to radars. Assumed optics requires Sun as a light source and this requirement indicates that space-based sensors should be located near SSO because such orbits provide almost steady optical environment between satellites and objects. And here, satellite lifetime is assumed as four years. This lifetime assumption affects orbital plane design.

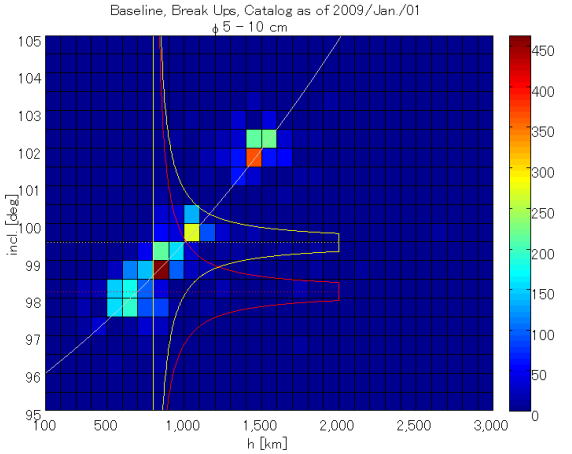

Figure 2. Objects distribution as a function of altitude and inclination and observable region for sweeping mission design

Fig. 2 describes small (5 to 10 cm) objects distribution around SSO as of 1st/January/2009. Horizontal axis is assumed altitude represented as $h = a - R_{\oplus}$, vertical axis is inclination. The reference debris environment in Fig. 2 is composed of actual tracking data, hypothetical data from historical breakup events and estimated environment baseline as of 1/Jan./2002. Objects' size information is not included in actual catalogue opened to the public in Two Line Elements (TLE) format. Therefore, these sizes are estimated using NASA Size Estimation Model (SEM) and apply SEM to Radar Cross Section (RCS) provided in satellite situation report [8] [1]. Objects with no available RCS value are assumed as 10 cm in size. Hypothetically generated data is based on confirmed on-orbit breakup event during 2002 to 2008 and fragments are generated by NASA standard breakup model 2001 revision [9] [10]

[11]. White curved line shows altitude and inclination relationship of circular SSO and it can be seen that near SSO region in altitude 800 to 1,000 km is one of the most congested areas. As a first step, target of orbit design for space-based sensor is defined as this area.

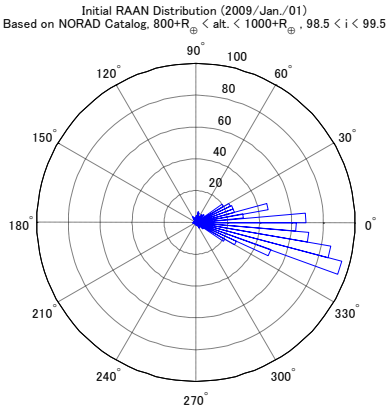

Figure 3. Initial condition of right ascension of the ascending node of actual catalogued objects in target area

Fig. 3 shows Right Ascension of the Ascending Node (RAAN) distribution at initial epoch and its parent population is objects in the most congested are in Fig. 2, altitude 800 – 1,000 km and inclination 98.5 – 99.5 degrees. It should be noted that this RAAN distribution refers only actual tracking catalogue with no size limitation. Because RAAN is relatively sensitive to perturbations in comparison to other elements such as altitude and inclination, at target altitude region and it is assumed that actual catalogue should have the most realistic RAAN data. Thus results shown in Fig. 3 cannot be used for observable objects number estimation however, it can apply for observable objects ratio prediction under an assumption that tracked objects represents orbital distribution trend of small objects. Fig. 3 indicates that object congestion in initial RAAN is located around -25 to 5 degrees and there are approximately 60 % of objects within the area enclosed by altitude 800 – 1,000 km and inclination 98.5 – 99.5 degrees. To enhance observation efficiency, observer satellite assumed to conduct sweeping observation along RAAN. Assumed sweep observation scenario is follows; 1) put an observer satellite into altitude 800 km near SSO with initial RAAN as -25 or 5 degrees (initial RAAN depends on drift rate condition) 2) sweep the congested RAAN region within four years.

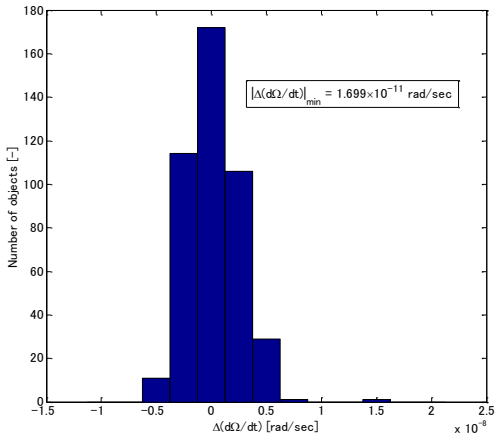

Figure 4. Difference of RAAN drift rate between ideal SSO and objects in congested initial RAAN region

Observer's orbit design based on the RAAN sweeping scenario should consider RAAN drift rate difference between observer and objects. Fig. 4 summarizes RAAN drift rate differences between ideal SSO object and objects in congested RAAN area in Fig. 3. It is concluded that observer in ideal SSO is not suitable for sweep observation with realistic mission duration according to this distribution. Because if a target with minimum RAAN drift rate difference is located 30 degrees away in RAAN at initial epoch, observer in ideal SSO requires approximately 1,000 years to reach the target orbital plane. To sweep 30 degrees width RAAN region in four years, observer satellite should have RAAN drift rate difference larger than 4.15×10^{-9}[rad/sec] in magnitude.

$$\dot{\Omega} = -\frac{3nR_{\oplus}^2 J_2}{2p^2}\cos i \tag{1}$$

Eq. 1 represents RAAN drift rate considering J_2 perturbation [12]. The altitude and eccentricity of observer should be fixed as 800 km and circular to maintain observable altitude region. Therefore the approach for sweep observation is based on inclination adjustment.

$$\begin{gathered} i_{obs} < 98.18\ [\text{deg}] \\ \text{or} \\ 99.48\ [\text{deg}] < i_{obs} \end{gathered} \tag{2}$$

Maximum and minimum drift rate difference in Fig. 4 and Eq. 1 derive requirement in observer inclination as shown in Eq. 2. Higher inclination orbital plane has RAAN drift rate enough faster than near SSO objects. In a similar way, lower inclination orbital plane has enough slower drift rates.

Here Field of View (FOV) and sensitivity analysis for observer should be conducted to evaluate observation

capability of space-based sensors. Optical device equipped on observer satellite is assumed as being composed of 2k2k cooled CCD and focal length 135 mm lens. This composition provides 12.9°×12.9° FOV. It is required to evaluate effect of relative position and velocity between observer and targets for sensitivity. Apparent motion furthermore brightness changes with relative condition. Target size and surface characteristics also affect brightness and these are assumed as 5 cm sphere with albedo 0.13 [13].

$$P_{in}[\text{count/pixel/sec}] \propto \frac{1}{\dot{\theta} \times \rho^2} \tag{3}$$

Incident photon count per pixel on CCD has inverse proportional relationship with apparent motion and relative distance as represented in Eq. (3). Observability of a target can be determined by proportional constant threshold value in Eq. (3) based on assumed optical device specifications.

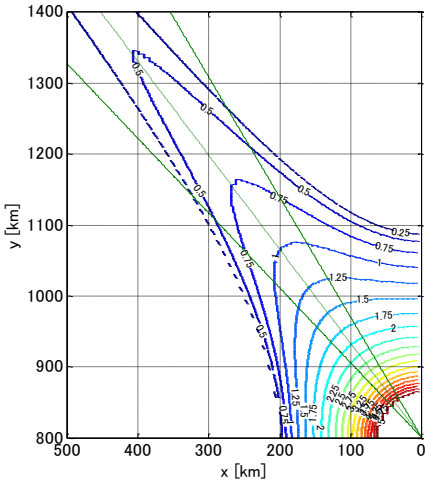

Figure 5. Observable orbital plane expressed as inclination difference on relative position plane

Observable objects' orbit is expressed as contour of inclination difference from observatory on relative position plane in Fig. 5. Horizontal axis is parallel to observer's velocity vector and vertical axis is parallel to observer's radial axis. Observer is located in $x = 0$, $y = 800$ [km]. Maximum inclination difference of observable orbital plane at each point in relative position plane is described as contour map. This result indicates that travelling direction and radial direction have disadvantages in different plane objects observation. Also it is found that elevation angle of 53 degree from travelling direction shows the most sensitive result for higher orbit objects. The green dashed line in Fig. 5 is the derived best elevation angle and two green lines are FOV boundary with assumed optics. Here FOV boundary for out-of-plane direction should be considered. Objects with difference inclination cannot be in a space-based sensor's FOV toward in-plane direction when the closest point is around polar region even if both orbits have same RAAN. This problem causes necessity of wide FOV in out-of-plane direction. The out-of-plane direction angle is defined as ±33° under the requirement not to miss the closest point of objects in orbital plane of 1,000 km altitude and 0.5 degrees in inclination difference. Therefore it is summarized that the observatory should equip six cameras with 12.9°×12.9° FOV along out-of-plane direction. Hereby maximum observable altitude for inclination differences in FOV is available and it enables to evaluate observable objects number. Observable altitude and inclination region for the observer located altitude 800 km and inclination 98.18 degrees is shown in Fig. 2 as an area enclosed by red line. And that of observer with inclination 99.48 degrees is also shown in Fig. 2 as enclosed area by yellow line. Note that mission objective is to track small objects in LEO therefore; altitude in observable region is limited to 2,000 km. Observable region illustrated on Fig. 2 clearly denote superiority of higher inclination 99.48 degrees orbit from a view point of enclosed objects number. Number of objects in yellow line shown in Fig. 2 is 1,945 and total number of objects within same size region in LEO is 9,997. Therefore it is found that potential observable objects ratio for observer located in altitude 800 km and inclination 99.48 degrees is approximately 20 % of LEO small objects. Observable objects number by sweeping observation with four years mission duration decreases approximately 60 % of potential observable objects under assumptions in initial RAAN distribution that tracked objects' trend represent that of faint objects. And higher inclination observer has faster RAAN drift rate than SSO thus observer's initial RAAN should be located in -25°. Thus conclusive number of observable objects within mission duration using single observer satellite is estimated as 1,114 and this is approximately 10 % of LEO small objects. Hereby initial guess capability from a view point of object number is found.

2.2 Ground Facilities

The last step of phase 1 in the whole mission geometry is to provide IOD results to ground facilities. It is required to evaluate whether or not IOD results are enough accurate to conduct ground based observation. To evaluate IOD accuracy in terms of apparent motion viewed from ground facilities, assumptions in observatories are required. The ground observatory network is assumed as being composed of three facilities; 1) Nyukasa observatory, Japan 2) Kiruna observatory, Sweden 3) NASA Orbital Debris Observatory (NODO), United States.

3 COLLABOLATION CAPABILITIES

The idea of collaborative observation is based on an assumption that the image stacking method is applicable for LEO objects with predicted apparent motions using initial orbit estimation result from space-based sensors. To verify the assumption, apparent motions of "true" and "estimated" trajectories is compared. The basis of apparent motion prediction is space-based angles only IOD with very short arc. Under such harsh conditions for orbit determination, classical IOD algorithm, e.g. Gaussian method, often makes large error in estimation results. Here, an algorithm with a limitation in eccentricity is defined as IOD method on space-based sensors. This limitation is not suitable for objects with high eccentricity such as geo transfer orbit. However, as previously mentioned, defined observation targets are almost circular SSO and it is assumed that the algorithm is effective for the objects. Collaborative observation capability evaluation is composed of following steps; 1) simulate space-based observation for the test case debris 2) conduct IOD with near circular constrained algorithm for simulated observation results 3) compare predicted apparent motion based on IOD results and true apparent trajectory. In simulations, debris and observers reference orbit is propagated by high precision numerical algorithm and true trajectory is based on reference orbit of debris.

Test case debris' principal orbital elements are follows; a = 7378.137 km, e =0.01, i = 100 deg. Also, observer satellite is located in 800 km altitude circular orbit with inclination 99.48 degrees according to sweep observation requirement analysis result. Errors in simulated observation are generated randomly and here, five times trial simulation is conducted. Observation angles errors are under Gaussian distribution assumption with 0.01 degrees for 1 σ. Position and velocity vectors errors for observer satellite are simulated by uniform distribution within ± 30 cm and 42 cm/s. These errors are based on specifications of optics, attitude determination sensors and Global Positioning System (GPS) receiver for satellites [13] [14]. To evaluate distribution in results caused by randomly generated errors, 5 time trials are conducted.

Table 1. Orbital elements at observation epoch

	a[km]	e[-]	i[deg]	Ω[deg]	ω[deg]	f[deg]
True	7395.2	0.01	100.0	10.80	342.2	201.0
1	7220.2	0.001	99.56	10.74	114.3	67.39
2	7362.1	0.001	99.81	10.77	114.4	68.25
3	7767.7	0.001	100.5	10.89	114.1	71.14
4	7195.3	0.001	99.53	10.73	114.3	67.25
5	7213.2	0.001	99.56	10.73	114.2	67.45

Tab. 1 describes angles only IOD accuracy using constrained algorithm with error contained data in very short arc (14 seconds). This result indicates that the IOD algorithm can estimate inclination and right ascension of the ascending node within 1 degree accuracy, i.e. orbital plane estimation accuracy is less than 1 degree. This is important result for apparent motion prediction because apparent trajectory is sensitive to errors in orbital planes. And it is assumed that errors in semi-major axis mainly affects to orbital period if the orbital plane is accurately determined. Orbital period error appears on apparent position as tangential direction difference. This difference can be shrunk by shortening the interval time between space-based IOD and ground tracking. Ground facility network is assumed to have a capability to shorten the interval.

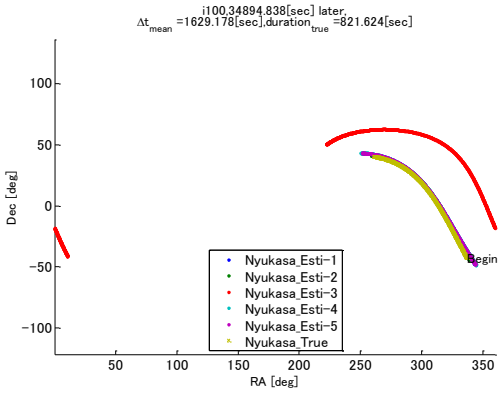

Figure 6. Apparent motion viewed from Nyukasa observatory

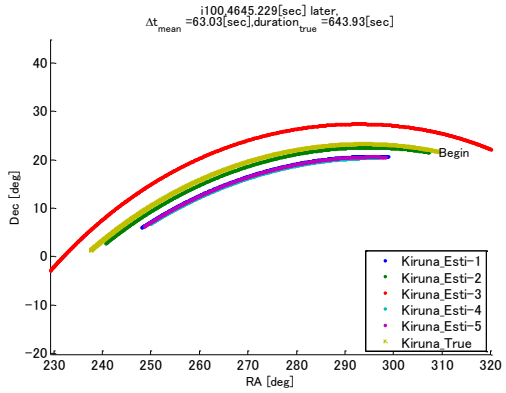

Figure 7. Apparent motion viewed from Kiruna observatory

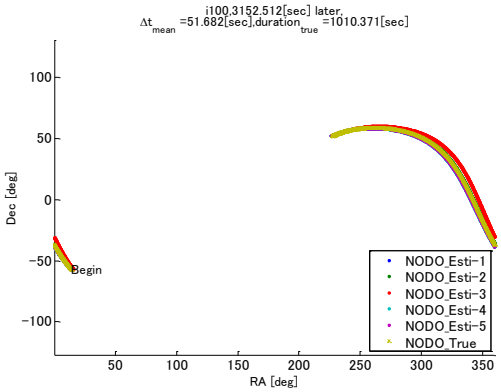

Figure 8. Apparent motion viewed from NODO

Fig. 6, 7 and 8 illustrate simulated first apparent motions for test cases and true orbit. Here "first" refers to first visible pass after space-based IOD and intervals of the IOD and first visible passes for ground are; 34,894 seconds (9.7 hours) for Nyukasa observatory, 4,645 seconds (77 minutes) for Kiruna observatory and 3,152 seconds (52 minutes) for NODO. Apparent trajectories in each ground facility are differs from true trajectory especially test case number 3 in Nyukasa observatory has large apparent difference. Apparent difference of other trajectories in Nyukasa observatory are relatively small however, there are disparities in observation epochs. Mean value of observation epoch differences between true and test cases in Nyukasa observatory is 1,629 seconds (27 minutes). Orbital periods of LEO objects are approximately 90 to 130 minutes therefore the epoch difference is more than 20 % of periods. With such large epoch difference, it is hard to identify and correlate objects between space-based IOD and ground observations. Other facilities have relatively small differences in apparent trajectories. Also mean epoch differences are smaller than that of Nyukasa observatory. Both differences are approximately a minute. This result confirms that effect of tangential errors in estimated orbit is behaves as a function of time and facility network is able to shrink the tangential direction error. And it seems that estimated trajectories are close to true one except trial 3 in Nyukasa observatory. However, it is also confirmed that apparent position errors between true and estimated orbits are tens of degrees in topocentric right ascension and inclination coordinate system. To cover whole of such difference, large FOV along estimated trajectories is required. The required FOV length along trajectories is approximately 40 degrees for Kiruna and approximately 80 degrees for NODO if trial 3 can be filtered. Otherwise FOV approximately 150 degrees length along trajectories is required. These summaries indicate possibility of collaborative observation while required FOV to cover whole trajectory is quite large. However further study in large error event is required such as occasion probability, conditions and recovery methods.

4 CONCLUSION

This paper proposed space-based short range observation for LEO small debris as a part of tracking capability improvement methods. Whole observation geometry proposed in this paper consists of the space-based sensor and the ground facility network. This collaborative observation geometry enables to detect objects smaller than 10 cm in LEO furthermore to track them. This paper discussed object detection capability of space-based sensor and feasibility of collaborative observation. The detection capability was evaluated using incident photon criterion according to optical device specifications. Also, observable conditions in orbital plane difference in terms of inclination were discussed. In association with this inclination discussion, this paper found observer's inclination criterion to sweep the congested region in initial RAAN. It is summarized that approximately 10 % of LEO small objects are potentially observable by single satellite located circular, altitude 800 km and near SSO inclination in four years. This paper also evaluated initial orbit estimation accuracy using space-based observation data. Test case results are based on very short arc, 14 seconds, observation and constrained orbit determination algorithm. Orbital planes of each case were estimated within 1 degree accuracy. On the other hand, results in semi-major axis had hundreds of km error. These facts indicated that estimated apparent trajectories might be almost overlapped to true one however, there are tangential directional errors. The tangential errors should increases as a function of time and this paper confirmed that ground facility network has a capability to shorten the tangential error because the network can shrink observation intervals. The minimum requirement to apply the image stacking method is containing true light spot in frames. It is summarized that 80 degrees length along trajectory and 20 degrees width in cross-track direction FOV is able to make true light point insight if anomalous value can be ignored. Otherwise 150 degrees length and 90 degrees width FOV is required. Therefore this paper concluded that it is possible to cover faint trajectory from ground facilities if the IOD results from space-based sensors and a large FOV are available. This detection capability indicates feasibility of ground-based tracking operation. However required FOV for ground observatories is quite large because the FOV is designed to cover whole trajectory. It should be studied minimum or optimal requirement in the FOV to make mission scenario more realistic. These results are based on assumptions such as image stacking method applicability toward LEO objects and object detection feasibility in images from space-based sensors. Apparent motion linearization should be mainly studied in image stacking method applicability evaluation.

REFERENCES

1. USSTRATCOM. Space-Track. Online at *https://www.space-track.org/* (as of 16 April 2013)
2. United Nations. (1999). Technical Report on Space Debris. United Nations Publication, New York, p15.
3. Christiansen, E. L. & Kerr, J. H. (2001). Ballistic Limit Equations for Spacecraft Shielding. *International Journal of Impact Engineering*. 26, 93-104.
4. Wesselius, P. R., Hees, R. v., Jonge, A. R. W. d., Roelfsema, P. R. & Viersen, B. (1993). Space Debris Observed by IRAS. *Adv. Space Res.* **13**(8), 49-57.
5. Gaposchkin, E. M., Braun, C. v. & Sharma, J. (2000). Space-based Space Surveillance with the Space-based Visible. *Journal of Guidance, Control and Dynamics*, **23**(1), 148-152.
6. Boeing. (2010). Space Based Space Surveillance Mission Book. Online at http://www.boeing.com/assets/pdf/defense-space/space/satellite/MissionBook.pdf (as of 16 April 2013).
7. Tagawa, M., Hanada, T., Yanagisawa, T., Matsumoto, H. & Kitazawa, Y. (2013). Low Earth Orbit Debris Observation Using Space-based Optical Sensors. (presented in *5th Space Debris Workshop*, Tokyo).
8. Yanagisawa, T. & Kurosaki, H. (2008). The Stacking Method: The Technique to Detect Small Size of GEO Debris and Asteroids. Japan Aerospace Exploration Agency.
9. Stokely, C. L., Foster, J. L., Stansbery, E. G., Benbrook, J. R. & Juarez, Q. (2006). The NASA Size Estimation Model. In *Haystack and HAX Radar Measurements of the Orbital Debris Environment; 2003*, JSC-62815, Lyndon B. Johnson Space Center, National Aeronautics and Space Administration. pp20-22
10. Johnson, N. L., Stansbery, E. G., Whitlock, D. O., Abercromby, K. J. & Shoots, D. (2008). History of On-orbit Satellite Fragmentations. Lyndon B. Johnson Space Center, National Aeronautics and Space Administration.
11. NASA. (2008). Satellite Breakups During First Quarter of 2008. In *Orbital Debris Quarterly News*, **12**(2). The NASA Orbital Debris Program Office. pp1-2.
12. Johnson, N. L., Krisko, P. H., Liou, J. –C. & Anz-Meador, P. D. (2001). NASA's New Breakup Model of EVOLVE 4.0. *Adv. Space Res.*, **28**(9), 1377-1384.
13. Vallado, D. A. (2007). Fundamentals of Astrodynamics and Applications, Springer, New York, US, pp. 851-858.
14. Mulrooney, M. & Matney, M. (2007). Derivation and application of a global albedo yielding an optical brightness to physical size transformation free of systematical errors. In *Proceedings of 2007 AMOS Technical Conference*, Kihei, HI, pp. 719-728.
15. Axelspace Corp. (2012). Star Sensor AxelStar-2. Online at *http://www.axelspace.com/en/developers/axelstar2-e.html* (as of 16 April 2013).
16. Spacelink Corp. (2011). GPS receiver for small-satellites IGPS-3. Online at *http://members.jcom.home.ne.jp/socrate/catalog_IGPS-3_spacelink.pdf* (as of 16 April 2013).